

## 1                                    **Electronic Supplementary Information**

### 2   **N-Carbamoylmaleimide-treated carbon dots: stabilizing the** 3   **electrochemical intermediate and extending for the ultrasensitive** 4   **detection of organophosphate pesticides**

5 Jinjin Xu,<sup>a</sup> Chaofan Yu,<sup>a</sup> Tao Feng,<sup>a,b</sup> Mingyue Liu,<sup>a</sup> Fengting Li,<sup>a,b</sup> Ying Wang\*<sup>a,b</sup> and Jingjuan  
6 Xu<sup>c</sup>

7 *a. Shanghai Key Lab of Chemical Assessment and Sustainability, College of Environmental*  
8 *Science and Engineering, School of Chemical Science and Engineering, Tongji University,*  
9 *Shanghai 200092, China.*

10 *b. Shanghai Institute of Pollution Control and Ecological Security, Shanghai 200092, P.R. China.*

11 *c. State Key Laboratory of Analytical Chemistry for Life Science, School of Chemistry and*  
12 *Chemical Engineering, Nanjing University, Nanjing 210023, China.*

13

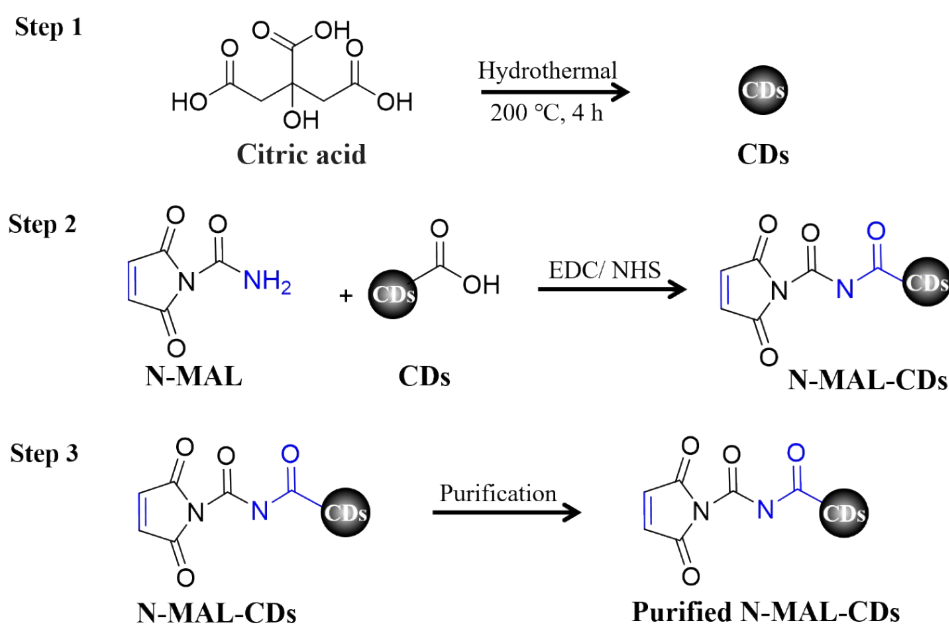
#### 14 **1. Preparation of CDs and N-MAL-CDs**

15        In the present work, N-MAL-CDs was synthesized based on N-MAL  
16 functionalized CDs, which was divided into three steps and shown in Fig. S1.

17        Step 1: CDs was synthesized following a standard hydrothermal procedure.<sup>1</sup> Citric  
18 acid (1.15 g) was dissolved in 15 mL water and then this solution was sealed into a  
19 Teflon-lined autoclave and heated at 200 °C for 4 h. After the autoclave was cooled to  
20 room temperature, the aqueous solutions were filtered and centrifuged at 6000 rpm for  
21 10 min to separate them from agglomerated larger particles.

22        Step 2: N-MAL was used to amidate with CDs through EDC/NHS catalysis to form  
23 derivatives of citrazinic acid. Finally the resulted solution was obtained and named N-  
24 MAL-CDs solution.

25        Step 3: Most unreacted reagents were removed through dialysis bag of 1000 D for  
26 24 h to purify N-MAL-CDs.



27

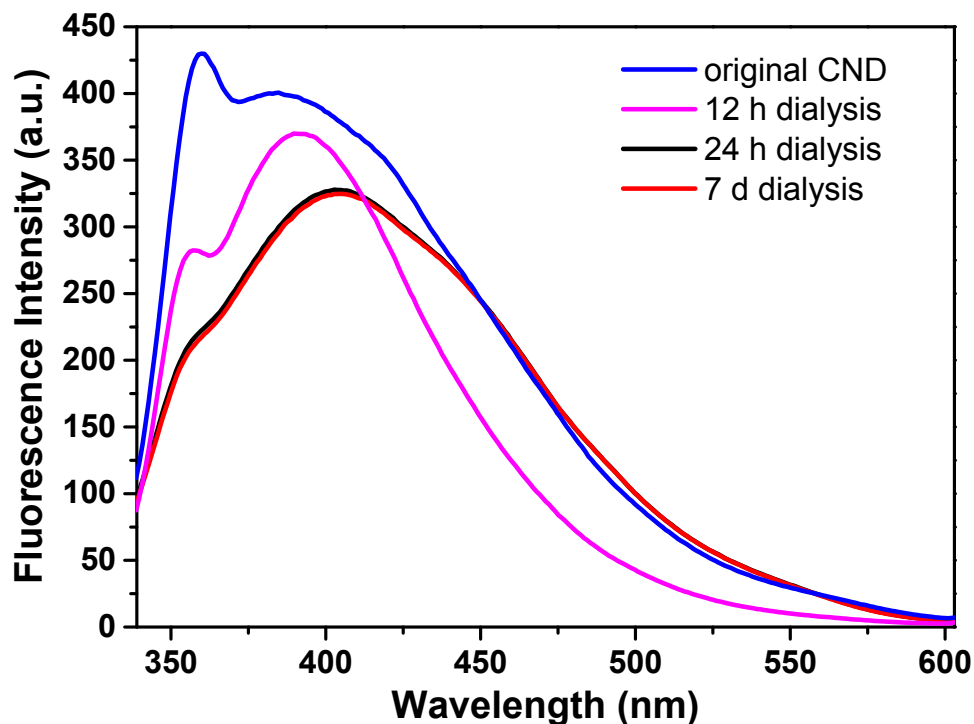
28 **Fig. S1** The process of forming CDs and N-MAL-CDs. Step 1: Citric acid was used for  
 29 producing CDs with hydrothermal method. Step 2: N-MAL was used to amidate with  
 30 CDs through EDC/NHS catalysis. Step 3: Purification by dialysis (24 h) for N-MAL-  
 31 CDs.

32

### 33 **2. Characterization of CDs and N-MAL-CDs**

34 Purification of the prepared CDs was implemented by using filtration,  
 35 centrifugation and dialysis in turn. CDs was filtered and centrifuged at 6000 rpm for 10  
 36 min to separate it from agglomerated larger particles, and then the product was  
 37 concentrated by the evaporation of water using rotary evaporation system. Afterwards,  
 38 the concentrated sample was put in dialysis of 1000 Da against deionized water for 24  
 39 h in order to remove most unreacted reagents.

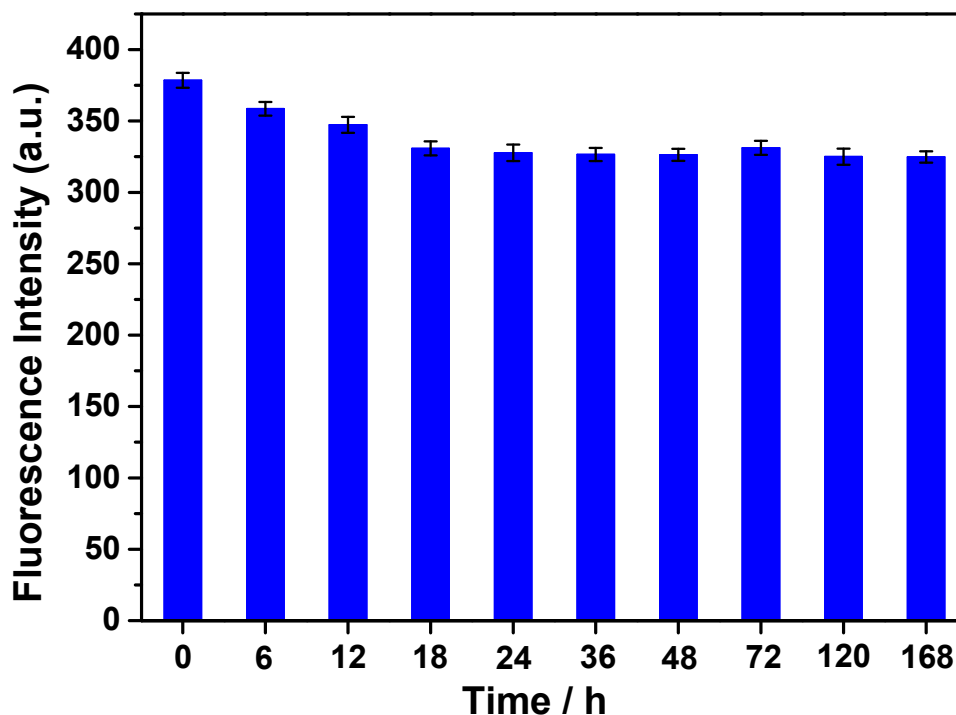
40 As shown in Fig. S2, black line is corresponding to 24 h dialysis and red line is  
 41 corresponding to 7 d dialysis. By comparing the results of 24 h and 7 d dialysis,  
 42 undesired impurities would be removed completely by 24 h dialysis. As shown in Fig.  
 43 S3, obvious changes about the fluorescent intensity can be noticed from the very  
 44 beginning to 18 h. However, no obvious fluorescent changes can be observed for the  
 45 purified CND after 1 d dialysis, as well as for the following every 24 h, until 168 h. The  
 46 fluorescence intensity is stable around 330 a.u. after 24 h dialysis.



47

48 **Fig. S2** Fluorescence emission spectra of CND that without dialysis (blue) and  
 49 subjected to dialysis for 12 h (magenta), 24 h (black) and 7 d (red) in aqueous solutions.

50

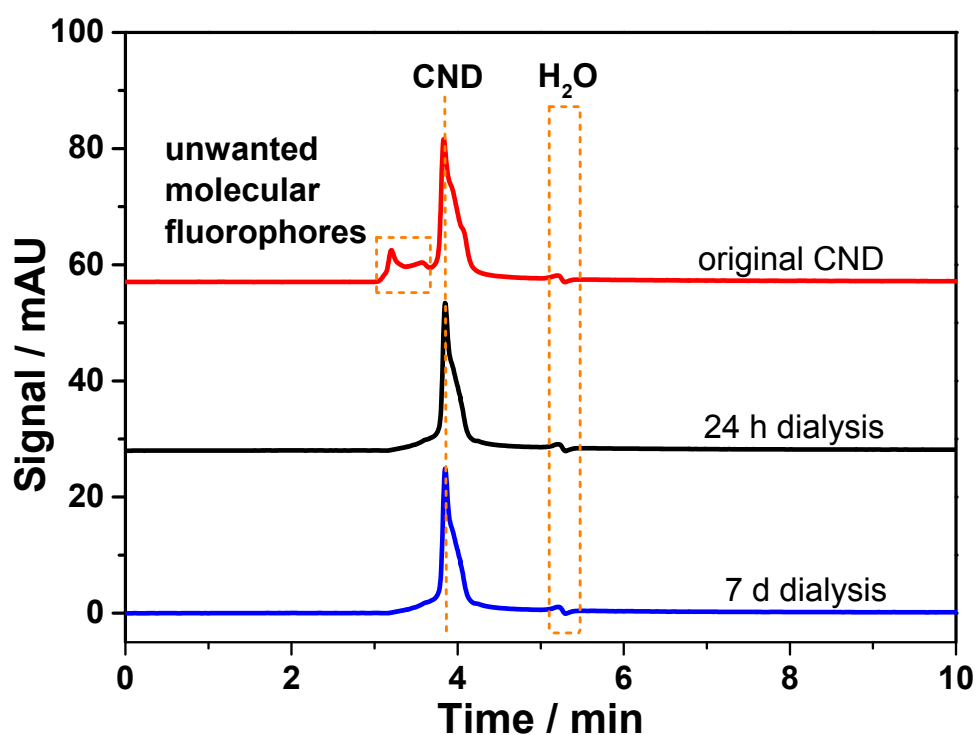


51

52 **Fig. S3** The fluorescence intensities of the CND under different dialysis time at the  
 53 fluorescent emission peak position of 405 nm.

54 To further demonstrate the purification results, we chose Agilent 1200 Infinity

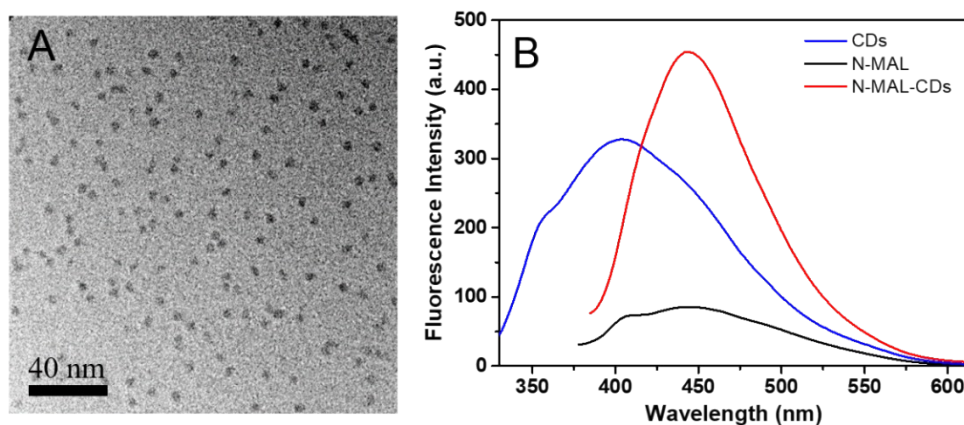
55 chromatograph to carry out the purification. Chromatographic separation of the  
56 prepared CDs was performed at 30 °C on Diamonsil C-18 column (5 μm, 250 ×4.6  
57 mm) using isocratic elution of acetonitrile-water (20:80, v/v) as mobile phase. Injection  
58 volume was 10 μL, and the flow rate was set at 0.6 mL/min. Chromatograms of original  
59 CDs (red line), 24 h dialysis CDs (black line) and 7 d dialysis CDs (blue line) are  
60 shown in Fig. S4. Only one chromatographic peak was observed for both 24 h and 7 d  
61 dialysis CDs, demonstrating the successful purification of CDs.



62  
63 **Fig. S4** HPLC chromatograms of CND that subjected to dialysis (1000 Da cut off) for  
64 0 h (black), 24 h (red) and 168 h (blue).

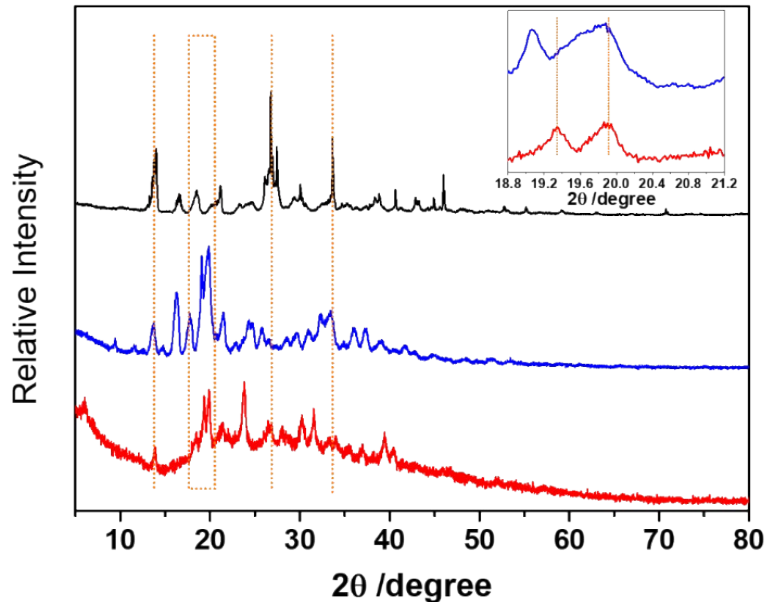
65 The CDs formation occurs through carbonization of the precursors at 200 °C and  
66 yields small particles, as the TEM images shown in Fig. S5A, indicating the carbon  
67 core was formed at the expense of the molecular fluorophores. N-MAL itself has a  
68 fluorescent phenomenon (Fig. S5B, black). When the amino group of N-MAL and the  
69 carboxyl group on the surface of CDs were amidated through EDC/NHS catalysis,  
70 organic fluorophores were introduced to the surface of CDs. So by comparing the  
71 emission spectra of those three kinds of materials (Fig. S5B), the fluorescence signal of  
72 N-MAL-CDs emitted is the synergistic effect of carbon core and organic fluorophores.<sup>2-</sup>  
73 <sup>8</sup> Briefly, the fluorescence signal of N-MAL-CDs emitted is the synergistic effect of

74 carbon core and organic fluorophores. So N-MAL-CDs is N-MAL functionalized CDs.  
75 There is organic fluorophore in the surface of N-MAL-CDs.  
76 XRD patterns of the N-MAL-CDs and purified N-MAL-CDs (Fig. S7) displayed a  
77 broad peak centered at  $2\theta = 24.2^\circ$ , which is also attributed to highly disordered carbon  
78 atoms.<sup>1,9</sup> In summary, the material is amorphous.



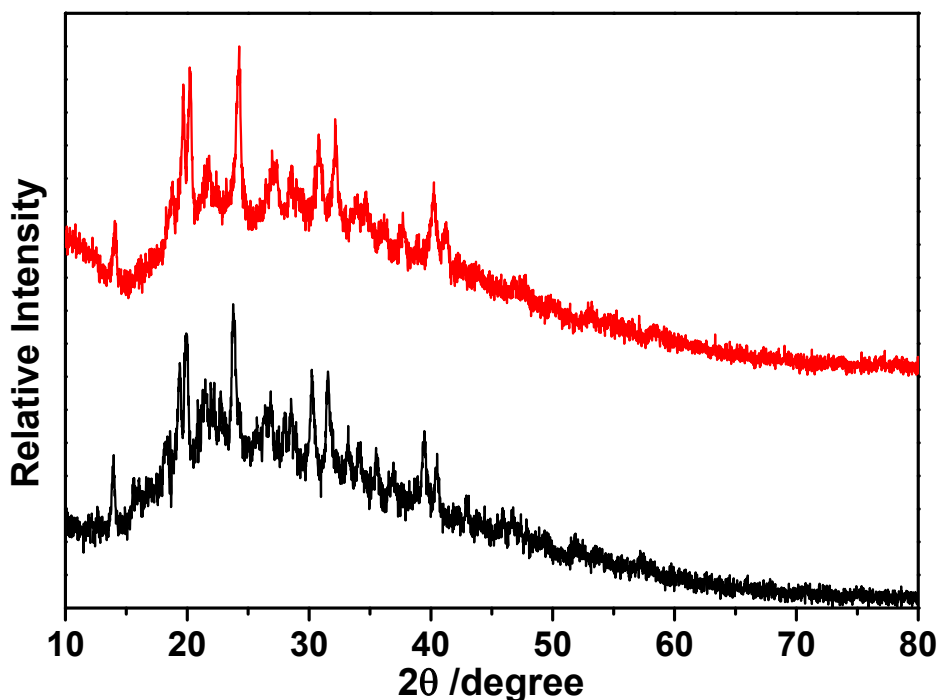
79

80 **Fig. S5** (A) TEM images of CDs. (B) Fluorescence emission spectra of N-MAL (black),  
81 CDs (blue) and N-MAL-CDs (red) in aqueous solutions.



82

83 **Fig. S6** XRD patterns of N-MAL (black), CDs (blue), and N-MAL-CDs (red). The  
84 dotted line is a guide for the eyes.



85

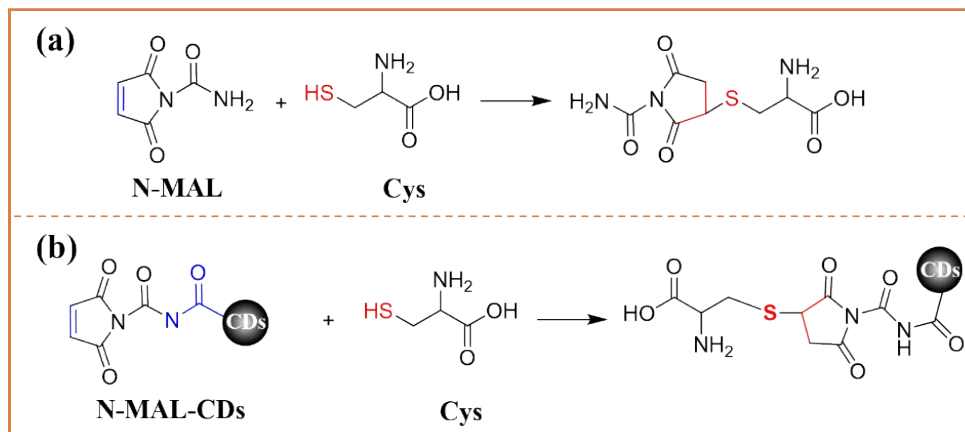
86 **Fig. S7** XRD patterns of N-MAL-CDs (red) and purified N-MAL-CDs (black).

87

### 88 **3. Fluorescence investigation of the occurrence of Michael addition**

89 The Michael addition reaction is a facile reaction between nucleophiles and  
 90 activated olefins or alkynes in which the nucleophile adds across carbon-carbon  
 91 multiple bonds. Therefore, Cysteine (Cys) that can provides a live -SH as a reactant  
 92 were chose to demonstrate the mechanism of Michael addition in this work. The  
 93 reaction schemes of N-MAL and Cys (a), N-MAL-CDs and Cys (b) toward the  
 94 formation of C-C-S based on Michael addition was shown in Scheme R1. As all known,  
 95 the change of fluorescence signals is due to the change of molecular structure. So the  
 96 fluorescence experiments were carried out to verify the mechanism, shown as Fig. S8.  
 97 It can be seen that a much higher fluorescence is observed for both N-MAL and N-  
 98 MAL-CDs upon addition of Cys, which means stable complexes were formed. The  
 99 good stability was considered from the chemical covalent-binding between C=C on N-  
 100 MAL-CDs derived from N-MAL and -SH from Cys to form C-C-S bond through

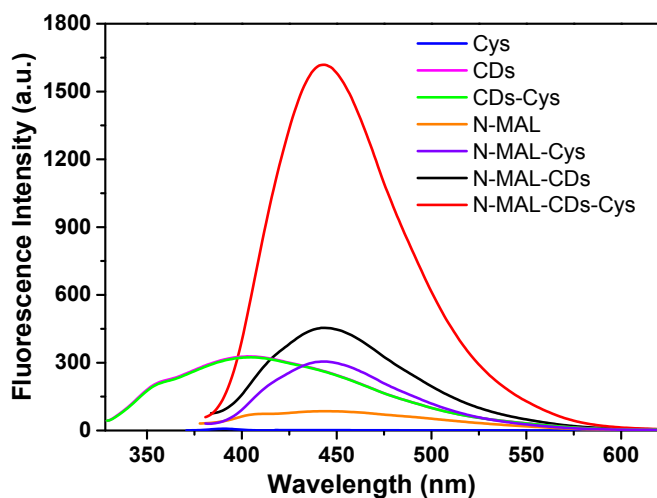
101 Michael addition. Moreover, there is no obvious change of fluorescence intensity of  
 102 CDs upon addition of Cy. By using fluorescence tests, Michael addition between N-  
 103 MAL-CDs and -SH containing group has been demonstrated.



104

105 **Scheme. S1** Schematic illustration of C-C-S formation based on Michael addition  
 106 between N-MAL and Cys (a), and N-MAL-CDs and Cys (b).

107



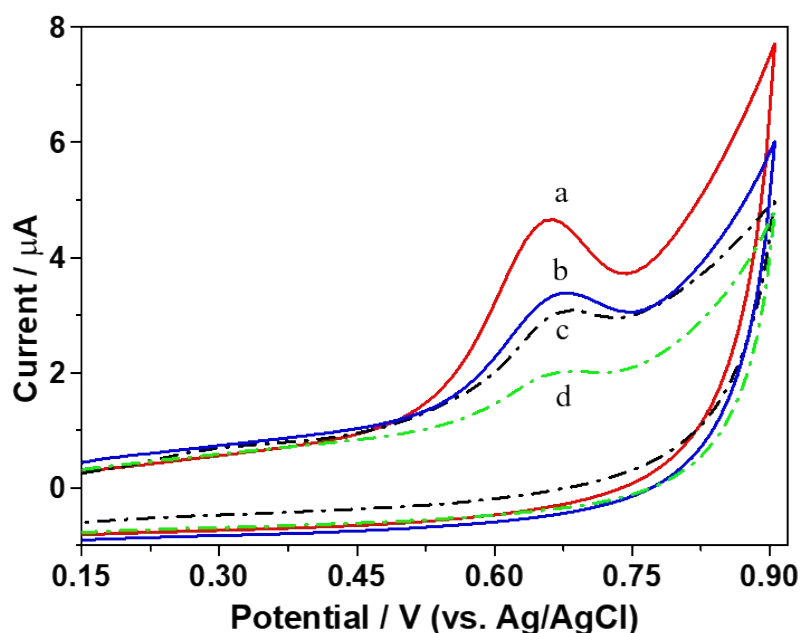
108

109 **Fig. S8** Fluorescence emission spectra of CD (green), N-MAL (violet) and N-MAL-  
 110 CDs (red) in the presence of 1.0 m M Cys in aqueous solutions (denoted as CDs-Cys,  
 111 N-MAL-Cys, N-MAL-CDs-Cys). Compared to the spectra of pure Cys aqueous  
 112 solution (blue), CDs aqueous solution (magenta), N-MAL aqueous solution (orange)  
 113 and N-MAL-CDs aqueous solution (black).

114

115 **4. Comparison of electrochemical performances of N-MAL-CDs and CDs for OPs**  
116 **detection**

117 The electrochemical performances of N-MAL-CDs and CDs for OPs detection  
118 were compared and the results are shown in Fig. S9. Fig. S9 displays a well-defined  
119 oxidation peak ( $E_{p_a}$  0.66 V) on AChE/N-MAL-CDs/SPE. The operation potential was  
120 negatively shifted 80 mV, and the electrochemical signals greatly increased with  
121 AChE/N-MAL-CDs modified SPE compared to AChE/CDs. The lower operation  
122 potential of 0.66 V and higher electrochemical current of 4.68  $\mu$ A demonstrated that  
123 the effect of N-MAL-CDs/SPE was stronger than CDs/SPE. When incubated with  
124  $1.6 \times 10^{-8}$  M parathion-methyl for 14 min firstly and then the same amount of ATCh as  
125 above was added, AChE would be inhibited and resulted in a decrease in the current  
126 response, and the results demonstrate that AChE/N-MAL-CDs shown higher sensitivity  
127 than AChE/CDs.



128

129 **Fig. S9** CVs of AChE/N-MAL-CDs (a), AChE /CDs (c), on the SPE in 0.01 M PBS  
130 containing 2 mM ATCh. CV of AChE /N-MAL-CDs/SPE (b) and AChE/CDs/SPE (d)  
131 in the presence of  $1.6 \times 10^{-8}$  M parathion-methyl in 0.01 M PBS.

132



133 **Table S1** Determination of parathion-methyl and paraoxon in tap water samples.

<b>Sample (tap water)</b>	<b>Taken (M)</b>	<b>Found (M)</b>	<b>Recovery (%)</b>
Parathion-methyl			
1	$1.9 \times 10^{-14}$	$2.1 \times 10^{-14}$	110.5
2	$3.8 \times 10^{-12}$	$3.9 \times 10^{-14}$	102.6
3	$3.8 \times 10^{-10}$	$4.1 \times 10^{-14}$	107.9
Paraoxon			
1	$3.6 \times 10^{-14}$	$3.5 \times 10^{-14}$	97.2
2	$3.6 \times 10^{-12}$	$3.7 \times 10^{-12}$	102.8
3	$3.6 \times 10^{-10}$	$3.9 \times 10^{-10}$	108.3

134

### 135 **References**

- 136 1. S. J. Zhu, Q. N. Meng, L. Wang, J. H. Zhang, Y. B. Song, H. Jin, K. Zhang, H. C.  
137 Sun, H. Y. Wang and B. Yang. *Angew. Chem.*, 2013, 125, 4045-4049.
- 138 2. M. J. Krysmann, A. Kelarakis, P. Dallas and Emmanuel P. Giannelis. *J. Am. Chem.*  
139 *Soc.*, 2012, 134, 2, 747-750.
- 140 3. J. B. Essner, J. A. Kist, L. Polo-Parada and G. A. Baker. *Chem. Mater.*, 2018, 30,  
141 1878-1887.
- 142 4. C.J. Reckmeier, J. Schneider, Y. Xiong, J. Häusler, P. Kasák, W. Schnick and A.L.  
143 Rogach. *Chem. Mater.*, 2017, 29, 10352-10361.
- 144 5. F. Ehrat, S. Bhattacharyya, J. Schneider, A.Löf, R. Wyrwich, A. L. Rogach, J. K.  
145 Stolarczyk, A. S. Urban and J. Feldmann. *Nano Lett.*, 2017, 17, 7710-7716.
- 146 6. S. Khan, A. Sharma, S. Ghoshal, S. Jain, M. K. Hazra and C. K. Nandi. *Chem. Sci.*,  
147 2018, 9, 175-180.
- 148 7. N. Nenadis and K. Stavra. *J. Phys. Chem. A*, 2017, 121, 2014-2021.
- 149 8. M. Righetto, A. Privitera, I. Fortunati, D. Mosconi, M. Zerbetto, M. L. Curri, M.  
150 Corricelli, A. Moretto, S. Agnoli, L. Franco, R. Bozio and C. Ferrante. *J. Phys.*  
151 *Chem. Lett.*, 2017, 8, 2236-2242.

152 9. X. Jian, X. Liu, H. Yang, J. Li, X. Song, H. Dai and Z. Liang, *Appl. Surf. Sci.*, 2016,  
153 370, 514-521.